The Journal of Immunology

Premature Terminal Exhaustion of Friend Virus-Specific Effector CD8 + T Cells by Rapid Induction of Multiple Inhibitory Receptors

Shiki Takamura, Sachiyo Tsuji-Kawahara, Hideo Yagita, Hisaya Akiba, Mayumi Sakamoto, Tomomi Chikaishi, Maiko Kato and Masaaki Miyazawa

J. Immunol. 2010;184;4696-4707; originally published online Mar 29, 2010;
doi:10.4049/jimmunol.0903478
http://www.jimmunol.org/cgi/content/full/184/9/4696

The Journal of Immunology is published twice each month by The American Association of Immunologists, Inc., 9650 Rockville Pike, Bethesda, MD 20814-3994.

Print ISSN: 0022-1767 Online ISSN: 1550-6606.

Premature Terminal Exhaustion of Friend Virus-Specific Effector CD8$^+$ T Cells by Rapid Induction of Multiple Inhibitory Receptors

Shiki Takamura,* Sachiyo Tsuji-Kawahara,* Hideo Yagita,† Hisaya Akiba,† Mayumi Sakamoto,* Tomomi Chikaishi,*,‡ Maiko Kato,*,§ and Masaaki Miyazawa*

During chronic viral infection, persistent exposure to viral Ags leads to the overexpression of multiple inhibitory cell-surface receptors that cause CD8$^+$ T cell exhaustion. The severity of exhaustion correlates directly with the level of infection and the number and intensity of inhibitory receptors expressed, and it correlates inversely with the ability to respond to the blockade of inhibitory pathways. Friend virus (FV) is a murine retrovirus complex that induces acute high-level viremia, followed by persistent infection and leukemia development, when inoculated into immunocompetent adult mice. In this article, we provide conclusive evidence that FV infection results in the generation of virus-specific effector CD8$^+$ T cells that are terminally exhausted. Acute FV-induced disease is characterized by a rapid increase in the number of virus-infected erythroblasts, leading to massive splenomegaly. Most of the expanded erythroblasts strongly express programmed death ligand-1 and MHC class I, thereby creating a highly tolerogenic environment. Consequently, FV-specific effector CD8$^+$ T cells uniformly express multiple inhibitory receptors, such as programmed cell death 1 (PD-1), T cell Ig domain and mucin domain 3 (Tim-3), lymphocyte activation gene-3, and CTLA-4, rapidly become nonresponsive to restimulation and are no longer reinvigorated by combined in vivo blockade of PD-1 and Tim-3 during the memory phase. However, combined blockade of PD-1 and Tim-3 during the priming/differentiation phase rescued FV-specific CD8$^+$ T cells from becoming terminally exhausted, resulting in improved CD8$^+$ T cell functionality and virus control. These results highlight FV's unique ability to evade virus-specific CD8$^+$ T cell responses and the importance of an early prophylactic approach for preventing terminal exhaustion of CD8$^+$ T cells. ***The Journal of Immunology*****, 2010, 184: 4696–4707.**

Viruses have acquired, through evolution, a multitude of strategies for evading immune surveillance and persisting in the host. A prominent example of such an evasion mechanism is the exhaustion of virus-specific CD8$^+$ T cells, which is caused by a continuous triggering of virus-specific TCRs owing to a high Ag load in persistently infected animals (1). Programmed cell death-1 (PD-1) has been identified as a major cell-surface inhibitory receptor that regulates CD8$^+$ T cell exhaustion (2). The levels of PD-1 expression on CD8$^+$ T cells critically correlate with Ag load and the severity of exhaustion (3–7). For example, in the case of hepatitis C virus infection, highly PD-1$^+$ and profoundly dysfunctional CD8$^+$ T cells were located at the sites where the relevant Ag persisted at high levels, such as the liver (8). Although blockade of PD-1/programmed death ligand (PD-L)1 interactions during the chronic phase of infection is a promising approach to reinvigorating the exhausted Ag-specific CD8$^+$ T cells, such an intervention resulted in little effect for these highly exhausted PD-1^{Hi} CD8$^+$ T cells (8, 9). A recent study using the lymphocytic choriomeningitis virus (LCMV) provided a likely explanation for the relatively limited effect of the PD-1 blockade: exhausted CD8$^+$ T cells are coregulated by multiple inhibitory receptors during chronic infection (10). Thus, targeting the precise inhibitory receptors for blockade (10–13), the timing and duration of treatment, and combination with additional therapeutic vaccination and/or antiviral drugs (14) must be considered to establish the optimal therapeutic strategy that can improve/restore the function of virus-specific CD8$^+$ T cells without enhancing immunopathology.

Friend virus (FV) is the pathogenic retrovirus complex comprising the replication-competent Friend murine leukemia helper virus (F-MuLV) and the replication-defective spleen focus-forming virus (SFFV). Although most other retroviruses, including Moloney murine leukemia virus, establish chronic infection only when they are inoculated into neonatal mice, FV is a unique virus that causes severe immunosuppression and establishes chronic infection, even when inoculated into immunocompetent adult mice (15). Comparative studies of these pathogens would lead to an understanding of the mechanisms of viral escape from host immune responses. FV uses a cationic amino acid transporter, which is expressed on most cell types (16–18), as an entry receptor, allowing this virus to infect a broad spectrum of cells in vivo. Upon inoculation, the virus replicates first in vascular endothelial cells and then reaches the actively dividing hematopoietic cells, including erythroid progenitor cells, a major target of FV infection in the bone marrow (19). The product of the SFFV *env* gene, gp55, then induces rapid proliferation and terminal differentiation of infected erythroid progenitor cells, resulting in massive splenomegaly within a few days

*Department of Immunology and §Department of Dermatology, Kinki University School of Medicine, Osaka-Sayama; †Department of Immunology, Juntendo University School of Medicine, Tokyo; and ‡Unmet Medical Needs Pharma, Yokohama, Japan

Received for publication October 26, 2009. Accepted for publication February 24, 2010.

This work was supported by grants-in-aid for scientific research from the Ministry of Education, Culture, Sports, Science and Technology of Japan, including the High-Tech Research Center project, and grants from the Ministry of Health, Labor and Welfare of Japan and the Japan Health Sciences Foundation (all to M.M.).

Address correspondence and reprint requests to Prof. Masaaki Miyazawa and Dr. Shiki Takamura, Department of Immunology, Kinki University School of Medicine, 377-2 Ohno-Higashi, Osaka-Sayama, Osaka 589-8511, Japan. E-mail addresses: masaaki@med.kindai.ac.jp and stakamura@immunol.med.kindai.ac.jp

Abbreviations used in this paper: B6, C57BL/6; F-MuLV, Friend murine leukemia virus; FV, Friend virus complex; LCMV, lymphocytic choriomeningitis virus; LDV, lactate dehydrogenase-elevating virus; nTreg, naturally occurring Treg; PD-1, programmed cell death 1; PD-L, programmed death ligand; SFFV, spleen focus-forming virus; Tim-3, T cell Ig domain and mucin domain 3; Treg, regulatory T.

www.jimmunol.org/cgi/doi/10.4049/jimmunol.0903478

postinfection (15, 20). This rapid and vigorous expansion of erythroid progenitor cells accelerates the viral replication that leads to the high-level viremia and provides a large pool of additional target cells for repeated integration of F-MuLV and SFFV proviruses. Ultimately, FV-infected mice develop erythroleukemia through promoter insertion or the silencing of a tumor suppressor gene (21) or, if able to recover from acute FV-induced disease, develop a life-long chronic infection (22).

Although it is well known that the control of Moloney murine leukemia virus infection largely depends on $CD8^+$ T cells (23), the actual contribution of virus-specific $CD8^+$ T cell responses to the control of FV infection is still controversial and inconclusive. Previous studies reported that although virus-specific $CD8^+$ T cells acquired effector functions at an early stage of infection, these cells displayed a profound functional impairment during the chronic phase (24–26). This virus-specific memory $CD8^+$ T cell dysfunction in the chronic phase has been attributed to suppression by virus-induced regulatory T (Treg) cells, because FV infection results in more Treg cells during the chronic phase (24). Support for these ideas has mainly come through an adoptive transfer approach by which TCR-transgenic $CD8^+$ T cells transferred into acutely infected mice developed proper effector function, whereas cells transferred into chronically infected animals showed weaker cytokine production (24). Another piece of evidence for Treg cell-mediated $CD8^+$ T cell dysfunction in chronically infected mice was that endogenous $CD8^+$ T cells in acutely infected mice produced significant amounts of granzymes, whereas the production of granzymes by $CD8^+$ T cells during the chronic phase of FV infection was much weaker (25, 26). Because these studies did not take into consideration the potentially differential priming conditions (e.g., Ag doses and inflammatory stimuli between the acute and memory phases of FV infection and the stages of $CD8^+$ T cell differentiation from effector to memory), it is unclear whether the dysfunction of FV-specific $CD8^+$ T cells is due solely to the presence of virus-induced Treg cells, as is when and how FV-specific $CD8^+$ T cells suffer functional defects throughout the entire course of FV infection. Furthermore, it has been confirmed that the FV stocks used in the above-reported studies were contaminated with lactate dehydrogenase-elevating virus (LDV), which has been shown to rapidly induce polyclonal T and NK cell activation and enhance Treg cell activities, resulting in delayed and suppressed FV-specific $CD8^+$ T cell responses (27). Taken together, understanding the precise mechanisms and the time course of virus-specific $CD8^+$ T cell dysfunction using LDV-free FV complex is required to fully elucidate the immune evasion strategy of FV.

In this study, we provide evidence that FV infection leads to the global unresponsiveness of virus-specific $CD8^+$ T cells, even during the early stages of infection. Owing to the massive erythroid cell proliferation caused by SFFV, the dysfunctional virus-specific effector $CD8^+$ T cells uniformly express multiple inhibitory molecules and are poorly responsive to the combined blockade of PD-1 and T cell Ig domain and mucin domain 3 (Tim-3), indicating that they are terminally exhausted. However, the combined blockade of PD-1 and Tim-3 during the priming/differentiation phase rescued virus-specific $CD8^+$ T cells from becoming terminally exhausted. These results demonstrate that FV successfully evades host $CD8^+$ T cell response by exploiting multiple negative regulatory pathways in its acute phase of infection.

Materials and Methods

Viruses, mice, cells, and infection

A stock of LDV-free B-tropic FV complex was kindly provided by Kim Hasenkrug, National Institutes of Health, National Institute of Allergy and Infectious Diseases, Rocky Mountain Laboratories (Hamilton, MT). FV was expanded, stored, and titered, as previously described (28). An infectious molecular clone of F-MuLV, FB29, was prepared from culture supernatant of chronically infected *Mus dunni* cells, as previously described (28). FBL3 is an F-MuLV–induced leukemia of C57BL/6 (B6) origin that expresses FV-related Ags and is known to be highly immunogenic; injection of 10^7 cells in syngeneic B6 mice results in rejection within 4 wk (29). C57BL/6CrSlc mice were purchased from Japan SLC (Hamamatsu, Japan). A/WySnJ mice were purchased from The Jackson Laboratory (Bar Harbor, ME). Animals were housed and bred in the experimental animal facilities at Kinki University School of Medicine under specific pathogen-free conditions. Male and female (B6 × A/WySnJ)F_1 mice, 6 to 10 wk old, were infected i.v. with 1000 spleen focus-forming units of FV or 1000 fluorescent focus units of F-MuLV. As a control, mice were injected s.c. with 5×10^6 FBL3. All animal studies were approved by Kinki University.

Tissue harvest and flow cytometry

Mice were sacrificed at the indicated time points, and single-cell suspensions of splenocytes were obtained by straining through nylon mesh, depleted of erythrocytes in buffered ammonium chloride, and panned on goat anti-mouse IgG (H+L) (Kirkegaard & Perry Laboratories, Gaithersburg, MD) for pentamer staining (30). Live-cell counts were determined by trypan blue exclusion. Isolated cells were incubated with anti-CD16/32 (BD Biosciences, San Jose, CA) for 15 min on ice to prevent test Abs from binding to FcRs and then stained with an allophycocyanin-labeled pentamer specific for an immunodominant F-MuLV *gag*-encoded MHC class I epitope CCLCLTVFL ($gag_{75–83}/D^b$) for 1 h at room temperature. Pentamer-labeled cells were then washed and stained with FITC-, PE-, PerCP/Cy5.5-, or APC-conjugated Abs for 30 min on ice. In some instances, cells were then fixed and permeabilized with the Cytofix Cytoperm kit (BD Biosciences) or FoxP3 Fix/Perm Buffer Set (BioLegend, San Diego, CA) to detect intracellular granzyme B (without in vitro restimulation) or FoxP3, respectively. The pentamer used was purchased from ProImmune (Oxford, U.K.). All three cysteine residues in the epitope peptide were replaced with aminobutyric acid to prevent interpeptide disulfide bonding (25). This variant peptide was shown to be recognized by $CD8^+$ T cells specific for $gag_{75–83}/D^b$ (25). Abs to the following molecules were purchased from BD Biosciences (CD3, CD4, CD8, Ter119, and CD11b), BioLegend (CD43 [1B11], CD25, PD-1, CD69, CD62L, CD122, CD127, Tim-3, LAG-3, CTLA-4, FasL, TRAIL, PD-L1, PD-L2, CD11c, and FoxP3), or Invitrogen (Carlsbad, CA; granzyme B). Purified anti–F-MuLV gp70 mAb, clone 720 (19), was labeled with biotin by NHS-PEG_4-Biotin (Thermo Scientific, Waltham, MA), as described (31). Labeled streptavidin was purchased from BioLegend. Samples were run on a FACSCalibur cytometer (BD Biosciences). All data were analyzed with FlowJo software (Tree Star, Ashland, OR).

In vitro restimulation and intracellular cytokine staining

Splenocytes isolated from infected mice, as described above, were incubated in a 96-well plate at a concentration of 1×10^6 cells per well. Cells were incubated in the presence of Alexa488-conjugated anti-CD107a, monensin A (BioLegend), and either $gag_{75–83}$ peptide (5 μM), FBL3 (1×10^5 cells/well), or anti-CD3 (4 μg/ml) (eBioscience, San Diego, CA) for 2 h at 37°C; brefeldin A (50 μg/ml) was added, and the incubation was continued for an additional 4 h. Surface staining for CD8 was performed as described above, and the cells were fixed and permeabilized with the Cytofix Cytoperm kit. For the detection of intracellular IFN-γ and granzyme B, the cells were incubated for 30 min in the Perm/Wash buffer followed by incubation in the same buffer with anti–IFN-γ and anti-granzyme B for 30 min; the cells were then washed and analyzed as described above. To correct for background variations between experiments, we subtracted the percentage of IFN-γ^+ or $CD107a^+$ cells among $CD8^+$ T cells without stimulation from the percentage of IFN-γ^+ or $CD107a^+$ cells following peptide stimulation, respectively, for each individual mouse.

Cytotoxicity assay

Fourteen days postinfection, splenocytes were depleted of erythroblasts using a magnetic depletion kit (Anti-mouse Ter119 Particles-DM; BD Biosciences) and further enriched for $CD8^+$ T cells using a negative selection kit (Mouse CD8 T Lymphocyte Enrichment Set-DM, BD Biosciences). Cells were then cocultured for 5 h with [^{51}Cr]-labeled EL-4 cells that had been loaded with $gag_{75–83}$ peptide. The ratio of $gag_{75–83}/D^b$-specific $CD8^+$ T cells to target cells (E:T ratio) was adjusted to 5:1. Frequencies of $gag_{75–83}/D^b$-specific $CD8^+$ T cells among purified cells were ~1.5% in each mouse, and spontaneous release was <1.4% in all experiments.

In vitro suppression assay

In vitro suppression assay was performed as described in a previous report, with minor alterations (32). $CD4^+CD25^+$ cells were sorted from the splenocytes of FV-infected or FBL3-injected mice at day 14. The frequency of $FoxP3^+$ cells among sorted cells in each group was ~68% for FV-infected mice and 95% for FBL3-injected mice. As a target, $CD44^{Hi}CD8^+$ splenocytes from naive mice were sorted and then labeled with 5 μM CFSE (Invitrogen). Cells were then combined

such that the numbers of FoxP3$^+$ and CD8$^+$ cells were equal and stimulated with anti-CD3 Ab (8 μg/ml). This ratio of Treg cells to CD8$^+$ target cells (1:1) is similar to that of total Treg cells to CD8$^+$ T cells specific for the single dominant FV epitope ($gag_{75–83}$) at day 14 in FV-infected mice (data not shown). For IFN-γ staining, brefeldin A (10 μg/ml) was added for the last 4 h of culturing. Six hours after stimulation, cells were stained for CD8, fixed, permeabilized, and stained for intracellular IFN-γ, as described above. Separate cultures of stimulated cells in the presence or absence of Treg cells were rested for 48 h to assess the CFSE dilution. Similar suppression between each group was also observed when the suppressor/target ratio was adjusted based on the number of CD4$^+$CD25$^+$ cells instead of FoxP3$^+$ cells (data not shown).

In vivo Ab blockade

Anti–PD-1 (250 μg; RMP1-14) (33), anti–Tim-3 (250 μg; RMT3-23) (34), anti–IL-10 (500 μg; JES5-2A5) (35), or control rat IgG (500 μg; Sigma-Aldrich, St Louis, MO) was administered i.p. every 3 d for 2 wk. The above doses of the blocking Abs used are sufficient to inhibit the relevant receptor–ligand interaction in vivo (36–38). RMP1-14 and RMT3-23 do not deplete PD-1– or Tim-3–expressing cells in vivo, and they have no agonistic activity (33, 34). For dual blockade of PD-1 and Tim-3, 250 μg each Ab was used.

Ligand-binding assay

Single-cell suspensions of splenocytes were obtained from Ab-treated mice, as described above. Blockade of PD-L1 interaction with PD-1 on the surface of CD8$^+$ T cells was measured by the ex vivo binding of the chimeric mouse B7-H1/Fc protein (R&D Systems, Minneapolis, MN). In brief, after FcR blocking, cells were incubated with the chimeric protein (1 μg/10^6 cells) for 1 h on ice and stained with anti-human IgG (Valeant Pharmaceuticals, Costa Mesa, CA), anti-CD8, and anti–PD-1 (RMP1-30), which is noncompetitive with RMP1-14. Because the Tim-3 ligand, galectin-9, can bind CD44, blockade of cell-surface Tim-3 was determined by the binding of fluorescent-conjugated anti–Tim-3 mAb (RMT3-23). Tim-3 expression on RMT3-23–treated cells was detected by using a different clone of anti–Tim-3 mAb (RMT3-8), which is noncompetitive with RMT3-23.

Infectious-center assays

Spleen cell suspensions were serially diluted and plated in duplicate at concentrations between 1×10^2 and 1×10^6 cells onto monolayers of *M. dunni* cells. After being washed and fixed with methanol on the second day of coculturing, cells were stained with biotinylated 720 mAb, and F-MuLV–infected foci were visualized using an Elite ABC Kit (Vector Laboratories, Burlingame, CA), as described (31).

Statistical analysis

One- and two-way ANOVA with Bonferroni or Dunnett posttests, as indicated, were used to determine statistically significant differences between groups of repeated measurements. For the comparison of groups or repeated measurements with different sample numbers, the Student or Welch *t* test was used, depending on whether variances were regarded as equal or not, and Bonferroni correction was used to determine α values based on the number of independent hypotheses. Prism software (GraphPad, San Diego, CA) was used to calculate *p* values.

Results

FV infection results in the generation of excessively activated CD8$^+$ T cells

Previous studies demonstrated that although FV infection elicits vigorous Ag-specific CD8$^+$ T cell responses, they are insufficient to totally eradicate FV-producing cells, and the virus persists after regression of acute splenomegaly even in the resistant strains, suggesting that FV-specific CD8$^+$ T cell responses are compromised during an early stage of infection (25). It has also become clear that FV stocks used in the previous studies were contaminated with LDV, which compromises CD8$^+$ T cell responses (27). To thoroughly investigate the potential factors that influence the onset of virus-specific CD8$^+$ T cell responses following FV infection in the absence of LDV, we compared the Ag-specific CD8$^+$ T cell responses elicited by FV infection or injection of FBL3 tumor cells, a highly immunogenic murine leukemia cell line induced in a B6 mouse by F-MuLV (39). As shown in Fig. 1*A*, FV infection elicited a robust virus-specific CD8$^+$ T cell response in the spleen at 14 d postinfection, with >5% of the CD8$^+$ T cell population stained brightly with the $gag_{75–83}/D^b$ pentamer. As a control, an s.c. injection of FBL3 elicited comparable numbers of $gag_{75–83}/D^b$-specific CD8$^+$ T cells at day 14 (Fig. 1*A*). However, despite the elicitation of comparable levels of acute CD8$^+$ T cell responses, there was a notable difference in the effector phenotypes between Ag-specific CD8$^+$ T cells elicited by FV infection and those elicited by FBL3 tumor injection. Although only less than one quarter of Ag-specific CD8$^+$ T cells generated by FBL3 injection displayed a highly activated effector phenotype, as determined by CD43 expression and intracellularly stored granzyme B, Ag-specific CD8$^+$ T cells generated by FV infection were markedly skewed toward the CD43$^+$/granzyme B$^+$ population; detection of this without in vitro restimulation (Fig. 1*B*) indicates that this was excessive. Substantial accumulation of granzyme B was also observed in the CD43^{Hi} population of $gag_{75–83}/D^b$-negative CD8$^+$ T cells in FV-infected mice, indicating that excessive activation is not a unique feature of $gag_{75–83}/D^b$-specific CD8$^+$ T cells. The frequency of CD8$^+$ T cells that contained granzyme B reached up to 48% of the total CD8$^+$ T cell population at 2 wk postinfection, and it declined after 3 wk postinfection (Fig. 1*C*). Importantly, this decrease in granzyme B expression was apparently associated with the course of virus elimination from the spleen (Fig. 1*D*). Because the expression of cytolytic molecules detected intracellularly without in vitro restimulation depends mainly on the recent Ag exposure in vivo (40), the reduction in granzyme B$^+$ cells through the late stage of infection is likely due to the combined consequences of the contraction of Ag-experienced effector

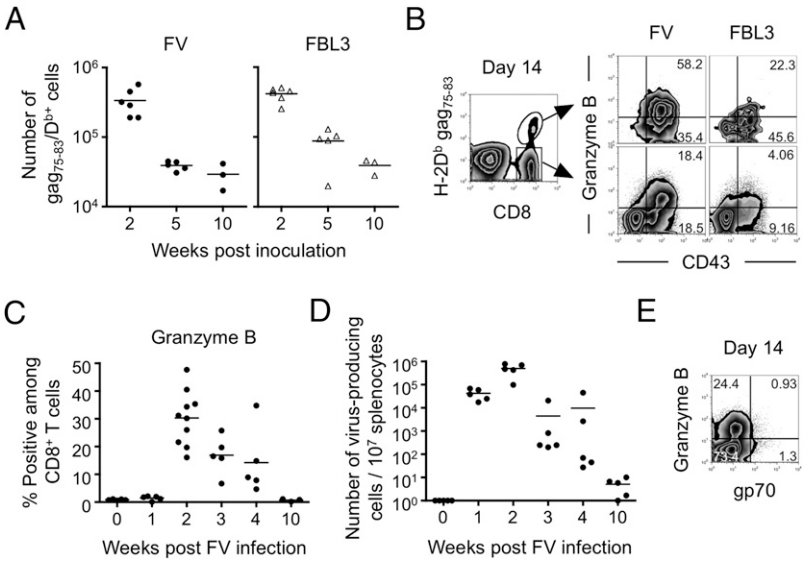

FIGURE 1. FV infection results in the generation of excessively activated CD8$^+$ T cells. Mice were infected with FV (1000 spleen focus-forming units) or injected with FBL3 (5×10^6 cells). Splenocytes were isolated at day 14 (*B*, *E*) or the indicated time points (*A*, *C*, *D*) and stained with Abs and/or FV $gag_{75–83}/D^b$ pentamer. *A*, Actual numbers of CD8$^+$/pentamer$^+$ cells in the spleen. *B*, Intracellular expression of granzyme B determined without in vitro restimulation. Shown are the representative staining patterns for CD43 and granzyme B of CD8$^+$/pentamer$^+$ or CD8$^+$/pentamer$^-$ cells at day 14. The numbers indicate the percentage of cells gated in each quadrant. *C*, Percentages of granzyme B$^+$ cells among splenic CD8$^+$ T cells. *D*, FV-producing infectious centers were enumerated by coculturing the splenocytes with *M. dunni* cells. Data are from the same experiment as in *C*. *E*, A representative staining pattern for gp70 and granzyme B of CD8$^+$ T cells. Numbers indicate the percentage in each quadrant. All data are representative of at least three independent experiments with essentially the same results.

$CD8^+$ T cells, the transition of $CD8^+$ T cells from effector to memory stages, and the resolution of FV infection in vivo. A relatively low number of $CD8^+$ T cells was positive for the virally encoded envelope protein (gp70), even at the peak of FV infection (Fig. 1*E*), indicating that direct infection of $CD8^+$ T cells with FV does not have much impact on the generation of excessively activated effector $CD8^+$ T cells.

FV-specific $CD8^+$ T cells are not responsive to restimulation

Because there is considerable evidence showing that $gag_{75–83}/D^b$-specific $CD8^+$ T cells generated by FBL3 injection are fully functional (39), it is of interest to compare the actual functionalities of $gag_{75–83}/D^b$-specific $CD8^+$ T cells generated by FV infection with those generated by FBL3 injection, especially during the early stages postinfection/injection. To do so, splenocytes from mice infected with FV or injected with FBL3 were cultured in vitro with $gag_{75–83}$ peptide for 6 h and evaluated for intracellular expression of IFN-γ and cell-surface expression of CD107a in conjunction with granzyme B expression. Upon peptide restimulation, $CD8^+$ T cells from FBL3-injected mice showed a significant increase in the intracellular expression of IFN-γ and the surface expression of CD107a at 2 and 3 wk after inoculation compared with those prior to the tumor injection (Fig. 2*A*, 2*B*). In contrast, $CD8^+$ T cells from FV-infected mice were nonresponsive to the restimulation; neither upregulation of cell-surface CD107a nor an increase in intracellular IFN-γ was observed (Fig. 2*A*). Surprisingly, we could not find any responses to the peptide restimulation during the entire course of FV infection (Fig. 2*B*), despite the presence of significant numbers of epitope-specific $CD8^+$ T cells (Fig. 1*A*). This contrasts remarkably with other models of chronic infection, such as infection with LCMV clone 13, in which virus-specific $CD8^+$ T cells still exhibit an ability to produce IFN-γ upon restimulation during the early stage of infection (10, 41). Furthermore, the excessively activated (granzyme B^+) $CD8^+$ T cell populations in FV-infected mice displayed severely impaired IFN-γ production even following anti-CD3 stimulation (Fig. 2*A*), suggesting that a vast majority of Ag-experienced $CD8^+$ T cells in FV-infected mice have a possible defect in TCR signaling. A strong staining for CD107a was observed intracellularly, supporting the notion that there was a defect in CD107a relocalization from intracellular lytic granules to the plasma membrane in response to TCR signaling in FV-infected mice (data not shown). The impaired responsiveness was not due to a dysfunction of APCs in the spleens of FV-infected mice, because similar results were observed even when restimulated with FBL3 (Fig. 2*A*). Thus, we hypothesized that although Ag-specific $CD8^+$ T cells from FV-infected mice expressed significant amounts of effector molecules, they were incapable of responding to the target, thereby failing to exert cytotoxicity. To directly test this, we performed ex vivo [^{51}Cr]-release assays. $CD8^+$-enriched splenocytes from FV-infected or FBL3-injected mice at day 14 were cocultured with $gag_{75–83}$ peptide-loaded EL-4 cells at an equivalent E:T ratio, based on the number of $gag_{75–83}/D^b$ pentamer$^+$ cells. As shown in Fig. 2*C*, virus-specific $CD8^+$ T cells from FV-infected mice exerted only marginal levels of cytotoxicity, whereas an equivalent number of virus-specific $CD8^+$ T cells from FBL3-injected mice exhibited significantly greater cytolytic activities. Collectively, these data provide convincing evidence that FV infection results in the generation of virus-specific effector $CD8^+$ T cells that are functionally impaired.

Minor contribution of Treg cells to the early loss of FV-specific $CD8^+$ T cell function

Given that infection of mice with FV plus LDV induced $CD4^+$ Treg cells that suppressed virus-specific $CD8^+$ T cells during the chronic phase of infection (24), we first considered the possibility that FV-induced Treg cells might contribute to the dysfunction of Ag-specific effector $CD8^+$ T cells. Because previous studies evaluated the presence of virus-induced $CD4^+$ Treg cells by the expression of CD25, we first compared the frequencies and the actual numbers of $CD4^+CD25^+$ T cells in the spleen between FV-infected

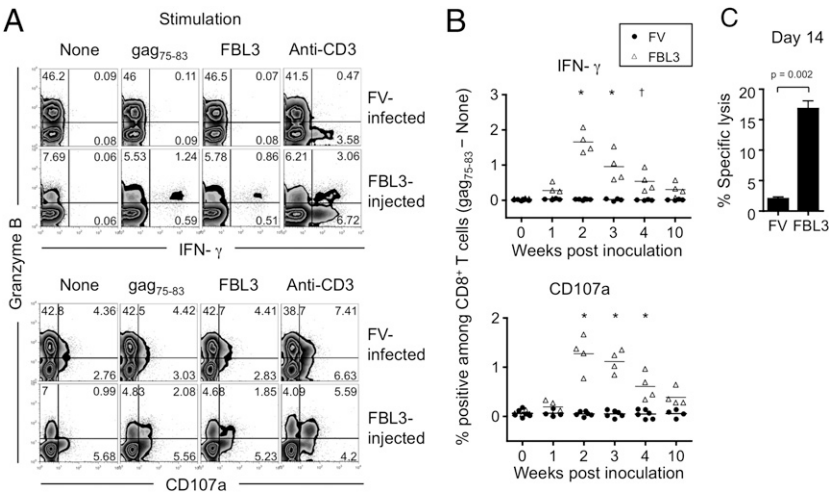

FIGURE 2. FV-specific $CD8^+$ T cells are not responsive to restimulation. Mice were infected with FV or injected with FBL3, as described for Fig. 1. *A*, Splenocytes were isolated at day 14 and stimulated with $gag_{75–83}$ peptide, FBL3, or anti-CD3 mAb for 6 h. The intracellular expression of IFN-γ and granzyme B and the surface expression of CD107a were measured by flow cytometry. Shown are representative staining patterns for granzyme B, IFN-γ, and CD107a of $CD8^+$ T cells. The numbers indicate the percentage of cells gated in each quadrant. As $CD8^+$ T cells were stimulated for 6 h in the presence of anti-CD107a Ab, granzyme B^-/$CD107a^+$ cells were observed, indicating degranulation. Data are representative of five independent experiments with essentially the same results. *B*, Ag-specific increase in the percentages of IFN-γ^+ and $CD107a^+$ cells among $CD8^+$ T cells calculated by (the percentage of IFN-γ^+ [$CD107a^+$] cells following peptide stimulation) − (the percentage of IFN-γ^+ [$CD107a^+$] cells without stimulation). Data are from the same experiment as in *A*. Each symbol represents an individual mouse. $*p < 0.001$; $^{\dagger}p < 0.01$ by two-way ANOVA, with Bonferroni posttests between the groups (FV versus FBL3). One-way ANOVA with Dunnett posttests indicated that the percentages of IFN-γ^+ and $CD107a^+$ cells at 2 and 3 wk after FBL3 injection were significantly higher than prior to injection ($p < 0.001$), and the percentage of $CD107a^+$ cells at 4 wk also was significantly increased ($p < 0.05$). *C*, Ex vivo cytotoxic activity of $gag_{75–83}/D^b$-specific effector $CD8^+$ T cells analyzed by [^{51}Cr]-release assay. Erythroblast ($Ter119^+$)-depleted splenocytes were further enriched for $CD8^+$ cells by negative selection. Cells were incubated with [^{51}Cr]-labeled EL-4 target cells that had been loaded with $gag_{75–83}$ peptide for 5 h. Data are representative of two independent experiments with essentially the same results. Bars indicate mean ± SEM.

and FBL3-injected mice. No significant groupwise differences were observed in the frequency or actual numbers of CD4$^+$CD25$^+$ cells between FV-infected and FBL3-injected mice, and the frequency and absolute numbers of CD4$^+$CD25$^+$ cells increased significantly from those before infection only at days 14 and 7 after FV infection, respectively (Fig. 3*A*, 3*B*). An additional phenotypic analysis showed that ~30% of the CD4$^+$CD25$^+$ cells in FV-infected mice were negative for FoxP3, whereas most of the CD4$^+$CD25$^+$ cells in FBL3-injected mice were FoxP3$^+$ (Fig. 3*C*, 3*D*). Moreover, a large majority of the FoxP3$^-$ CD4$^+$CD25$^+$ cells in FV-infected mice displayed highly activated phenotypes, as determined by the expression of PD-1 and CD69 (Fig. 3*C*, 3*D*), suggesting that the increased numbers of activated cells, but not an increase in Treg cells, were responsible for the slightly elevated levels of CD4$^+$CD25$^+$ T cells after FV infection. In fact, the actual numbers of FoxP3$^+$ Treg cells in FV-infected mice at day 14 were not different from those in FBL3-injected mice (Fig. 3*E*). To exclude the possibility that Treg cells from FV-infected mice possess higher suppressive ability than those from FBL3-injected mice, we performed in vitro suppression assays. Splenocytes from FV-infected or FBL3-injected mice were flow cytometrically sorted on the basis of CD4 and CD25 expression, and CD8$^+$ T cells were stimulated in the presence or absence of Treg cells, such that the ratio of CD8$^+$ cells to FoxP3$^+$ Treg cells was 1:1, >5-fold higher Treg cell density compared with the physiological condition. Treg cells from FV-infected mice showed a significant suppression of CD8$^+$ T cell functions but no increase in their suppressive ability compared with those from FBL3-injected mice (Fig. 3*F*). Taken together, we conclude that the observed early dysfunction of effector CD8$^+$ T cells in FV-infected mice is not explained by the Treg cell-mediated suppression.

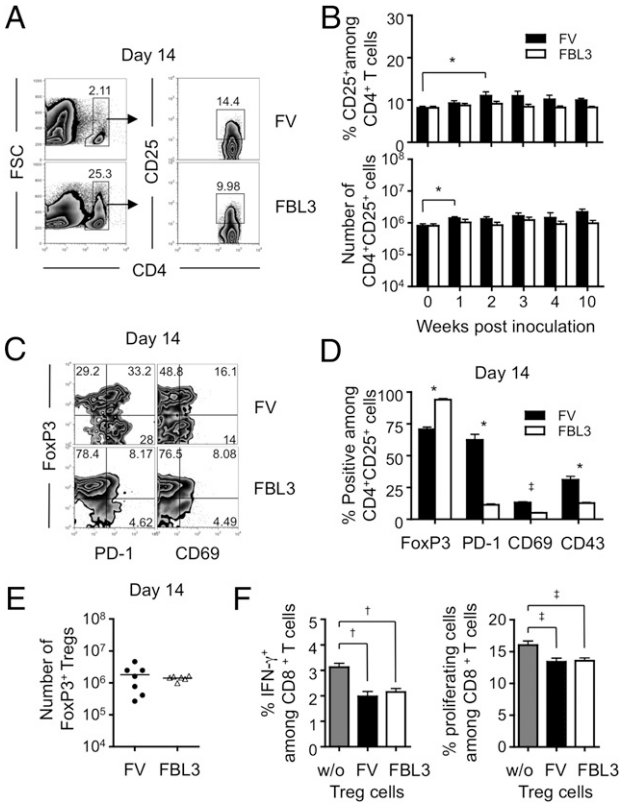

FIGURE 3. Minor contribution of Treg cells to the early loss of FV-specific CD8$^+$ T cell function. *A*, Representative staining patterns of CD4 and CD25 in FV-infected or FBL3-injected mice at day 14. *B*, Frequencies of CD25$^+$ cells among CD4$^+$ T cells and the actual numbers of CD4$^+$CD25$^+$ cells in the spleen at the indicated time points after FV infection or FBL3 injection. Bars indicate mean ± SEM. Because the number of samples at each time point differs, *t* tests with Bonferroni correction for the number of hypotheses were performed. *Significant increase from day 0 by $p < \alpha$ ($n = 5$) = 0.0102. *C*, Relative expression of activation markers (PD-1 and CD69) and the Treg cell marker (FoxP3) on CD4$^+$CD25$^+$ cells in the spleen of FV-infected or FBL3-injected mice. Profiles shown are of gated CD4$^+$CD25$^+$ cells. *D*, Phenotypic differences of CD4$^+$CD25$^+$ cells in FV-infected and FBL3-injected mice. Frequencies of the cells positive for the indicated markers among CD4$^+$CD25$^+$ cells in the spleen at day 14 are shown. *$p < 0.001$; ‡$p < 0.05$ by two-way ANOVA with Bonferroni posttests. *E*, Actual numbers of CD4$^+$CD25$^+$FoxP3$^+$ cells in the spleen of FV-infected or FBL3-injected mice at day 14. *F*, CD8$^+$ T cells were stimulated in vitro by anti-CD3 in the presence or absence (w/o) of Treg cells separated from FV-infected or FBL3-injected mice at day 14 and evaluated for intracellular IFN-γ expression (6 h) and proliferation (48 h). Data are representative of two independent experiments with essentially the same results. †$p < 0.01$; ‡$p < 0.05$ by one-way ANOVA with Bonferroni posttests.

FV-specific CD8$^+$ T cells show highly exhausted phenotypes

It is well established that virus-specific CD8$^+$ T cells eventually become dysfunctional during chronic diseases as the result of increased expression of inhibitory receptors, including PD-1. To test whether this could be the case for the observed dysfunction of FV-specific effector CD8$^+$ T cells in FV-infected mice, we analyzed the surface expression of PD-1 on the gag$_{75–83}$/D^b-specific CD8$^+$ T cells. Strikingly, as early as 14 d after FV infection, nearly all gag$_{75–83}$/D^b-specific CD8$^+$ T cells expressed high levels of PD-1 (Fig. 4*A*). Such a high expression of PD-1 on the gag$_{75–83}$/D^b-specific CD8$^+$ T cells was maintained until ≥10 wk postinfection (Fig. 4*B*). In contrast to other models of chronic

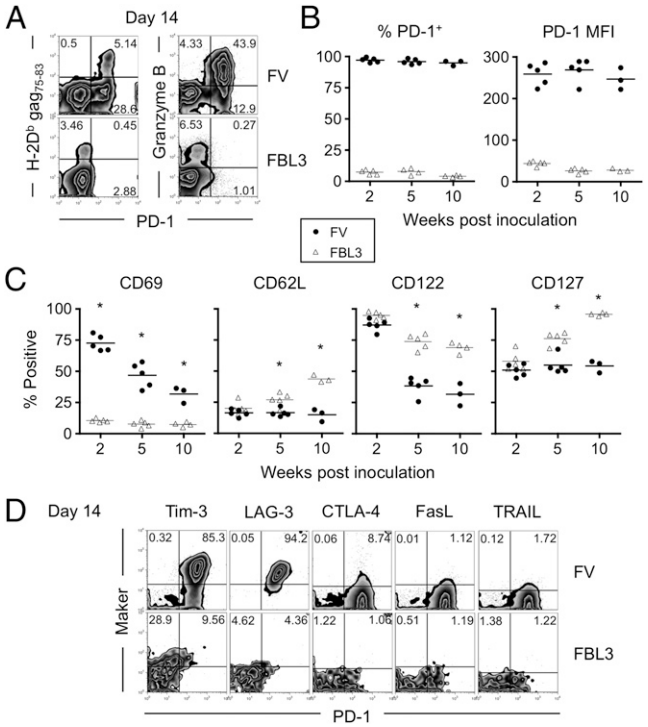

FIGURE 4. FV-specific CD8$^+$ T cells show highly exhausted phenotypes. *A*, Relative levels of PD-1 expression and the pentamer binding on CD8$^+$ T cells and their granzyme B contents in the spleens of FV-infected or FBL3-injected mice at day 14. Profiles shown are of gated CD8$^+$ T cells. *B* and *C*, Expression of the indicated surface molecules was assessed on gag$_{75–83}$/D^{b+} CD8$^+$ T cells at the indicated time points after FV infection or FBL3 injection. Each symbol represents an individual mouse. *$p < \alpha$ ($n = 3$) = 0.017 by two-tailed *t* test with Bonferroni correction. *D*, Representative FACS plots showing the coexpression of inhibitory molecules with PD-1 on gag$_{75–83}$/D^{b+} CD8$^+$ T cells in FV-infected and FBL3-injected mice at day 14. Profiles shown are of gated gag$_{75–83}$/D^{b+} CD8$^+$ T cells. All data are representative of at least three independent experiments with essentially the same results.

infection in which the expression levels of PD-1 on exhausted CD8$^+$ T cells were heterogeneous, Ag-specific CD8$^+$ T cells in FV-infected mice were predominantly PD-1^{Hi}, regardless of the stage of infection (Fig. 4*B*), revealing a unique severity of exhaustion caused by FV infection. Highly elevated expressions of PD-1 were also observed in the entire population of CD8$^+$ T cells that contained granzyme B in FV-infected mice (Fig. 4*A*), suggesting that a vast majority of Ag-experienced CD8$^+$ T cells, not just those specific for the gag$_{75–83}$ epitope, shared a propensity for severe exhaustion. Additional phenotypic profiles of Ag-specific CD8$^+$ T cells in FV-infected mice included higher expression levels of CD69 and lower expression of all three of the other markers (CD62L, CD122, and CD127) in comparison with those in FBL3-injected mice, revealing typical characteristics of exhaustion (Fig. 4*C*) (41). To more thoroughly pursue the severity of exhaustion, Ag-specific CD8$^+$ T cells were examined for the expression of additional inhibitory receptors. Concomitant with the elevated expression of PD-1, gag$_{75–83}$/D^b-specific effector CD8$^+$ T cells from FV-infected mice expressed three other cell-surface inhibitory receptors at high levels: Tim-3, LAG-3, and CTLA-4; this expression was obviously distinct from CD8$^+$ T cells with the same epitope specificity in FBL3-injected mice (Fig. 4*D*). A lack of the elevated expression of FasL and TRAIL suggests that these cells are not yet programmed to undergo activation-induced cell death (Fig. 4*D*). Taken together, these data suggest that the severe exhaustion of Ag-specific CD8$^+$ T cells occurs even in the early stage of FV infection.

Elevated expression of PD-L1 and MHC class I on FV-infected erythroblasts

The pronounced expression of PD-1 on FV-specific effector CD8$^+$ T cells prompted us to investigate the impact of FV infection on the expression of PD-1 ligands: PD-L1 and PD-L2. In contrast to a modest influence of FV infection on PD-L2 expression, significant upregulation of PD-L1 was observed in subpopulations of CD11b$^+$ dendritic cells and erythroblasts at 14 d after FV infection (Fig. 5*A*). The elevated expression of PD-L1 on erythroblasts was of particular interest because of the rapid expansion of these cells in the early phase of FV infection. In fact, the percentage of Ter119$^+$ erythroblasts among nucleated splenocytes increased to 75%, with a >45-fold increase in their number at its peak, which was accompanied by the expansive increase in FV-infected cells (Fig. 5*B*). Because an engagement of PD-1 and concomitant TCR stimulation, but not the engagement of PD-1 alone, is necessary for providing the negative signal to T cells (42), we further examined the possible expression of MHC class I molecules on the erythroblasts. In agreement with the previous findings that inflammatory stimuli activate hematopoiesis, resulting in increased numbers of nucleated erythroblasts that express MHC class I molecules (43), elevated expression of H-2D^b was even observed on the surfaces of erythroblasts from FBL3-injected mice (Fig. 5*C*). However, in the case of FV infection, nearly all expanded erythroblasts were positive for H-2D^b (Fig. 5*C*). Visualization of the erythroid cell expression of PD-L1 and viral protein revealed that ~50% of virus-infected cells were PD-L1^{Hi} (Fig. 5*D*). Together, these results suggest that the FV-infected erythroblasts can be a potent provider of PD-1–mediated negative signals to CD8$^+$ T cells.

Exhaustion of virus-specific CD8$^+$ T cells is irreversible in FV-infected mice

Thus far, the data have demonstrated that virus-specific CD8$^+$ T cells are exposed to abundant cell-associated viral Ags and immunosuppressive signals; therefore, they are highly exhausted at the early stage of FV infection. To determine whether the functionally exhausted CD8$^+$ T cells could be revived by a blockade of immunosuppressive signals, we attempted to interrupt two pathways by administering

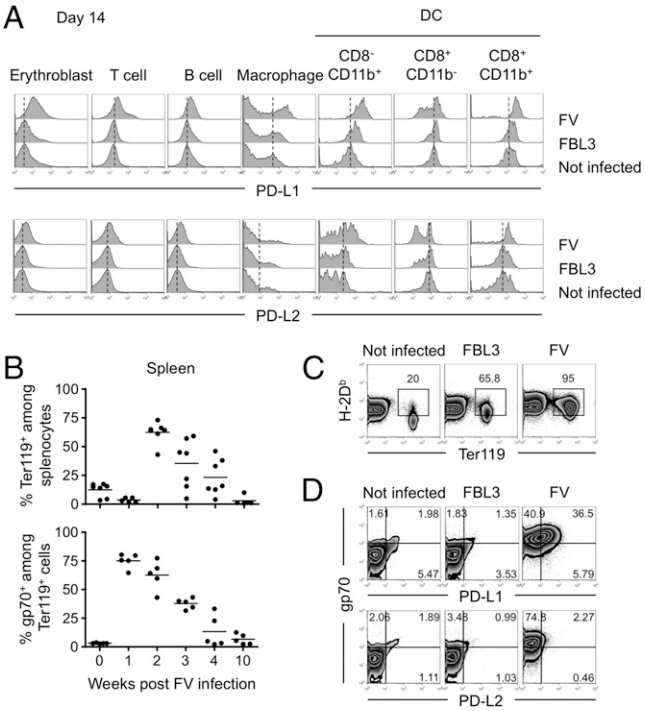

FIGURE 5. Elevated expression of PD-L1 and MHC class I on FV-infected erythroblasts. *A*, Expression of PD-L1 and PD-L2 was assessed on the indicated populations of spleen cells at 14 d after FV infection or FBL3 injection. Each population was defined as follows: erythroblasts, Ter119$^+$; T cells, CD3$^+$; B cells, CD19$^+$; macrophages CD11b$^+$CD11c$^-$; and DC, CD11c$^+$. *B*, Kinetic analyses of the frequencies of Ter119$^+$ cells and virus-infected erythroblasts in the spleen. *C*, Upregulation of MHC class I molecule on the erythroblasts 14 d after FV infection or FBL3 injection. The numbers indicate the percentage of H-2D^{b+} cells among Ter119$^+$ erythroblasts. *D*, Levels of expression of PD-1 ligands on FV-infected erythroblasts at day 14. Profiles shown are of gated Ter119$^+$ cells. All data are representative of at least three independent experiments with essentially the same results.

blocking Abs to PD-1 and Tim-3, alone or in combination. In the initial experiments, in vivo blockade was started at day 14 (Fig. 6*A*), when most Ag-specific CD8$^+$ T cells had already expressed these inhibitory receptors at high levels (Fig. 4). Despite the effective blockade of these inhibitory receptors on cell surfaces (Fig. 6*B*), no reversal of exhaustion was observed, even when in vivo blockade was performed by a combination of anti–PD-1 and anti–Tim-3 (Fig. 6*C*, 6*D*). Furthermore, the combined blockade of PD-1 and Tim-3 had no impact on the pathogen control, because the numbers of virus-producing spleen cells detected in the Ab-treated mice were similar to those in the control mice (data not shown). The failure of reinvigoration was probably not caused by the presence of abundant Ags during the blockade, because FV-specific memory CD8$^+$ T cells were still in the nonresponsive state, even when the blockade was operated between days 28–42 postinfection, when initial splenomegaly had regressed (data not shown). Given that CD8$^+$ T cell production of IFN-γ is the last function to be ablated in the stepwise hierarchy of T cell exhaustion (1), it is tempting to hypothesize that high-level viral replication in FV-infected mice results in the generation of terminally exhausted FV-specific effector CD8$^+$ T cells at a very early stage.

Acute SFFV-induced pathogenesis is responsible for the terminal exhaustion of effector CD8$^+$ T cells in FV-infected mice

We next asked whether SFFV-induced acute pathogenesis causes the terminal exhaustion of effector CD8$^+$ T cells in FV-infected animals. To test this, we examined the severity of CD8$^+$ T cell exhaustion in

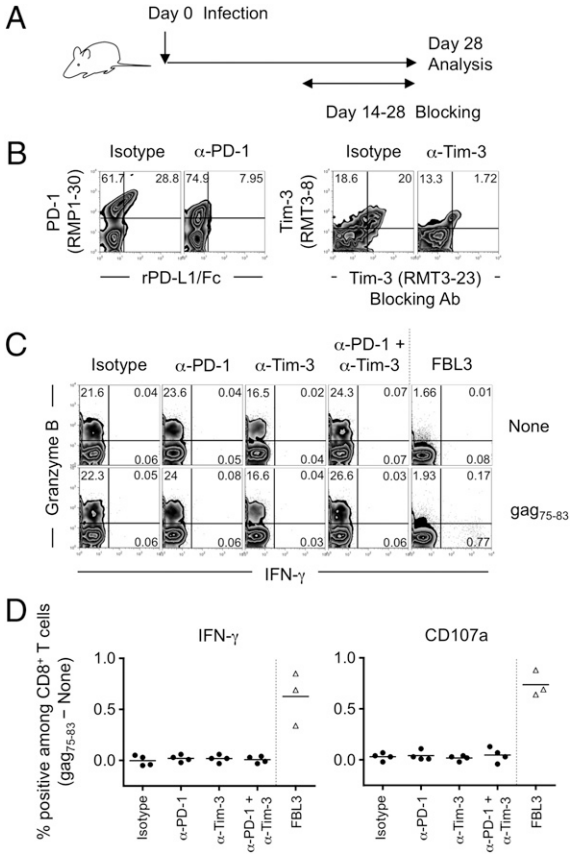

FIGURE 6. Exhaustion of virus-specific CD8$^+$ T cells is irreversible in FV-infected mice. *A*, Protocol for receptor blockade in the late phase of infection. Fourteen days after FV infection or FBL3 injection, isotype-matched control IgG, anti–PD-1 (RMP1-14), anti–Tim-3 (RMT3-23), or anti-PD-1 plus anti–Tim-3 was administered i.p. every third day for 2 wk. *B*, Splenocytes were isolated from FV-infected and Ab-treated mice at day 28, and the binding of specific ligand (PD-L1/Fc for PD-1) or clone-matched mAb (RMT3-23 for Tim-3) was assessed simultaneously with binding of noncompetitive mAbs against PD-1 (RMP1-30) or Tim-3 (RMT3-8), respectively. Plots shown are of gated CD8$^+$ T cells. The numbers indicate the percentage of cells gated in each quadrant. *C* and *D*, Twenty-eight days postinfection/injection, splenocytes were stimulated in vitro with $gag_{75–83}$ peptide or left unstimulated, and the intracellular expression of IFN-γ and granzyme B and surface expression of CD107a were measured by flow cytometry. *C*, Representative staining patterns for granzyme B and IFN-γ of CD8$^+$ T cells. The numbers indicate the percentage of cells gated in each quadrant. *D*, Ag-specific increase in the percentages of IFN-γ$^+$ and CD107a$^+$ cells among CD8$^+$ T cells. All data are representative of two independent experiments with essentially the same results.

mice infected with F-MuLV alone. At the peak of infection, FV infection induced severe splenomegaly due to the massive expansion of virus-infected erythroid progenitor cells, whereas such pathologies were not observed in mice infected with F-MuLV (Fig. 7*A*). Although ~25% of erythroid cells were infected with F-MuLV, these cells did not show any increase in the expression of PD-L1 (Fig. 7*B*), indicating that infection with F-MuLV alone results in a less immunosuppressive environment compared with that created by infection with FV complex. In the absence of the SFFV-induced acute pathogenesis, we noted a significantly reduced frequency and intensity of PD-1 expression on $gag_{75–83}/D^b$-specific CD8$^+$ T cells in F-MuLV-infected mice compared with those observed in FV-infected animals (Fig. 7*C*). When we examined the coexpression of inhibitory molecules with PD-1, PD-1$^+$ $gag_{75–83}/D^b$-specific CD8$^+$ T cells in F-MuLV–infected mice expressed less Tim-3, LAG-3, and CTLA4 than did FV-infected mice (Fig. 7*D*). CD8$^+$ T cells from F-MuLV–infected mice displayed a significantly lower accumulation of granzyme B without restimulation than that observed in FV-infected mice (Fig. 7*E*). These results suggest that high-level virus replication and/or erythroid cell proliferation induced by SFFV accelerates the expression of multiple inhibitory receptors on CD8$^+$ T cells that cause reduced functionality (8, 10). As expected, CD8$^+$ T cells from F-MuLV–infected mice responded to restimulation with $gag_{75–83}$ by producing significantly higher levels of IFN-γ than did the cells from FV-infected animals (Fig. 7*E*). Nevertheless, the levels of IFN-γ production were modest compared with those exhibited by CD8$^+$ T cells from FBL3-injected mice (Fig. 2*B*), indicating partial exhaustion of CD8$^+$ T cells in F-MuLV–infected mice. Using the same blocking approach as described for Fig. 6, we then asked whether the functions of partially exhausted CD8$^+$ T cells in F-MuLV–infected mice could be restored (Fig. 7*F*). As shown in Fig. 7*G* and 7*H*, treatment with anti–PD-1 alone that was started at day 14 significantly improved Ag-specific IFN-γ production from and CD107a mobilization on CD8$^+$ T cells, indicating that exhaustion of CD8$^+$ T cells in F-MuLV–infected mice was reversible. In contrast, blockade of Tim-3 alone had little effect on the functions of CD8$^+$ T cells (Fig. 7*G*, 7*H*), which is likely due to the relatively low expression of Tim-3 on $gag_{75–83}/D^b$-specific effector CD8$^+$ T cells (Fig. 7*D*). Taken together, these results suggest that SFFV causes rapid terminal exhaustion of virus-specific CD8$^+$ T cells by creating a highly tolerogenic environment.

Simultaneous blockade of PD-1 and Tim-3 pathways during priming/differentiation phase rescues CD8$^+$ T cells in FV-infected mice from becoming terminally exhausted

Because high-level expression of PD-1 can be observed by the time of first cell division under the tolerogenic environment (44), and the massive expansion of FV-infected erythroid cells begins as early as 1 wk postinfection (45), it is possible that Ag-specific CD8$^+$ T cells rapidly enter the state of full functional exhaustion during the priming/differentiation phase in FV-infected animals. To examine this, we next treated FV-infected mice with Abs to PD-1 and Tim-3 between days 2–14 postinfection, thereby attempting to ensure that virus-specific CD8$^+$ T cells were primed and differentiated in the absence of negative signals from these inhibitory receptors (Fig. 8*A*). As shown in Fig. 8*B* and 8*C*, blockade of PD-1 or Tim-3 alone during the initial priming modestly improved the ability of Ag-specific CD8$^+$ T cells to secrete IFN-γ upon peptide restimulation, indicating that both of these molecules contributed, at least in part, to the FV-specific CD8$^+$ T cell dysfunction. Importantly, a combined blockade of PD-1 and Tim-3 resulted in a significantly higher percentage of IFN-γ–producing CD8$^+$ T cells in response to gag_{75-83} peptide stimulation, which is comparable to the responses of CD8$^+$ T cells from FBL3-injected mice (Fig. 8*B*, 8*C*). These Ag-specific effector CD8$^+$ T cell populations that escaped terminal exhaustion were now able to establish memory CD8$^+$ T cell pools capable of producing IFN-γ upon restimulation in the later stage (Fig. 8*D*). Despite the effectiveness of dual blockade, nearly all $gag_{75–83}/D^b$-specific effector CD8$^+$ T cells still remained positive for PD-1 (Fig. 8*E*); however, the intensity of PD-1 on effector CD8$^+$ T cells was significantly decreased in mice simultaneously treated with PD-1 and Tim-3 (Fig. 8*E*), supporting the previous finding that the expression levels of PD-1 dictate the functional ability of CD8$^+$ T cells (9). In agreement with the enhanced functionality of Ag-specific effector CD8$^+$ T cells, we observed significantly improved viral control and reduced splenomegaly in mice simultaneously treated with PD-1 and Tim-3 (Fig. 8*F*). The analysis of total $gag_{75–83}/D^b$-specific CD8$^+$ T cell numbers revealed that, despite the quantitatively identical CD8$^+$ T cell responses during the early stage of infection (data not shown), dual blockade of PD-1 and Tim-3 resulted in the maintenance of substantially higher numbers of memory CD8$^+$ T cells at 10 wk postinfection (Fig. 8*G*), which is likely due to a significantly improved survival ability of Ag-experienced CD8$^+$ T cells, as indicated by the significantly reduced expression of

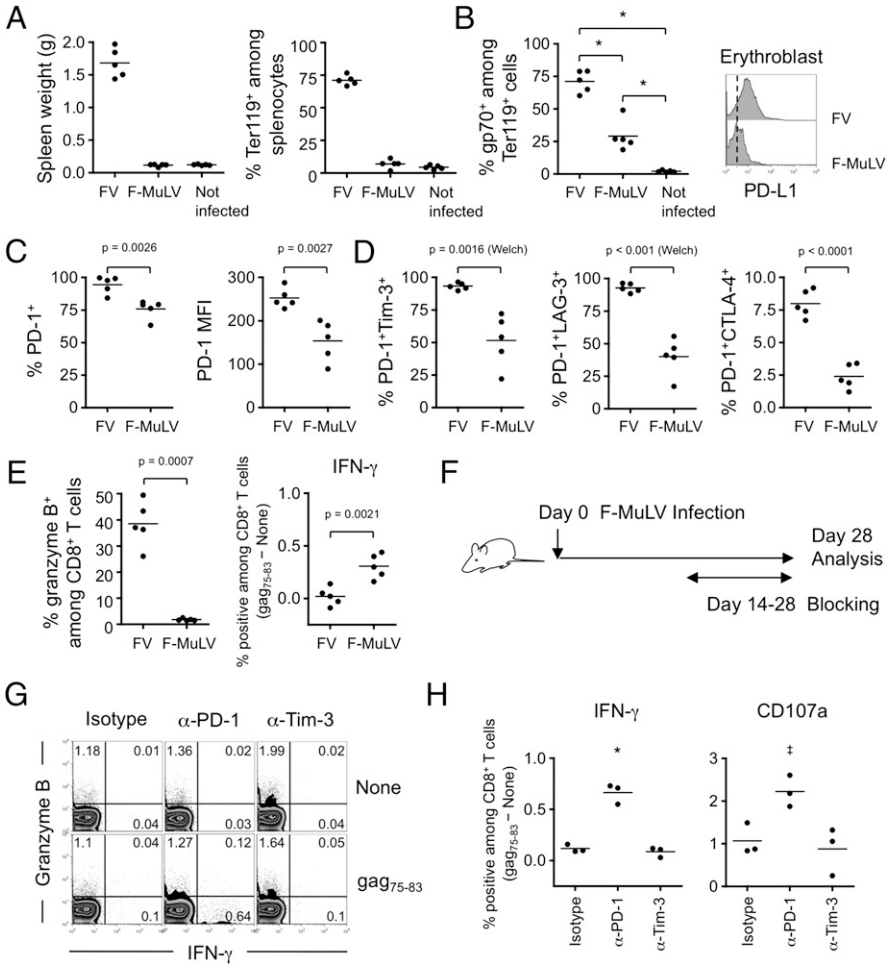

FIGURE 7. Acute SFFV-induced pathogenesis is responsible for the terminal exhaustion of effector $CD8^+$ T cells in FV-infected mice. Mice were inoculated with similar infectious titers of FV or F-MuLV alone. *A*, Spleen weight (*left panel*) and the percentage of $Ter119^+$ cells among splenocytes (*right panel*) at day 14 postinfection. Each symbol represents an individual mouse. *B*, Percentage of $gp70^+$ cells among $Ter119^+$ cells in the spleen at day 14 postinfection. $*p < 0.001$ by one-way ANOVA with Bonferroni posttests. Histograms indicate the expression levels of PD-L1 on the erythroblasts of FV- or F-MuLV–infected mice at day 14. *C* and *D*, Expression of the indicated surface molecules was assessed on $gag_{75–83}/D^{b+}$ $CD8^+$ T cells at day 14 postinfection. Groupwise differences were statistically examined by the Student or Welch *t* test. *E*, The percentage of granzyme B^+ cells among $CD8^+$ T cells without in vitro restimulation (*left panel*) and Ag-induced increase in the percentages of IFN-γ^+ and $CD107a^+$ cells among $CD8^+$ T cells (*right panel*) at day 14 postinfection. *F*, Protocol for receptor blockade at the late phase of F-MuLV infection. Fourteen days after F-MuLV infection, isotype-matched control IgG, anti–PD-1 (RMP1-14), or anti–Tim-3 (RMT3-23) was administered i.p. every third day for 2 wk. *G* and *H*, Twenty-eight days postinfection, splenocytes were stimulated in vitro with $gag_{75–83}$ peptide or left unstimulated, and the intracellular expression of IFN-γ and granzyme B and the surface expression of CD107a were measured by flow cytometry. *G*, Representative staining patterns for granzyme B and IFN-γ of $CD8^+$ T cells. The numbers indicate the percentage of cells gated in each quadrant. *H*, Ag-induced increase in the percentages of IFN-γ^+ and $CD107a^+$ cells among $CD8^+$ T cells. All data are representative of two independent experiments with essentially the same results. $*p < 0.001$; $^‡p < 0.05$ compared with isotype control by one-way ANOVA with Dunnett posttests.

Annexin V on their surfaces at day 14 (Fig. 8*H*). Finally, in contrast to the model of LCMV clone 13 infection (46–48), blockade of IL-10 during the early stage of infection had no impact on the responsiveness of FV-specific effector $CD8^+$ T cells or the viral clearance, indicating that FV-specific effector $CD8^+$ T cell exhaustion occurred in an IL-10–independent fashion (Fig. 8*B–F*). Overall, these data demonstrate that, in contrast to F-MuLV infection, infection with FV complex induces a massive expansion of virus-infected $PD\text{-}L1^{Hi}$ and MHC class I^+ erythroblasts during the priming/differentiation phase, and virus-specific effector $CD8^+$ T cells rapidly succumb to terminal exhaustion through accelerated high-level expression of multiple inhibitory receptors.

Discussion

It is well established that chronic Ag exposure leads to the stepwise functional exhaustion of $CD8^+$ T cells (1, 41). The cells lose the ability to produce IL-2, exert cytolysis, and proliferate in early stages of exhaustion, followed by the loss of TNF-α production. IFN-γ production is eventually compromised in the final stage of exhaustion. Although this hierarchical loss of effector functions takes place during the initial phase of chronic infection and causes the failure in viral clearance, terminal exhaustion of Ag-specific $CD8^+$ T cells is observed exclusively in the late stages of infection (41). In this study, we have revealed an exception to the above stepwise exhaustion: following FV infection, $gag_{75–83}/D^b$-specific effector $CD8^+$ T cells rapidly lose their ability to produce IFN-γ, a function most resistant to being lost, even during the early stage of infection. $CD8^+$ T cells specific for an immunodominant epitope are generally more prone to functional exhaustion than are those specific for other less-immunogenic epitopes, resulting in the inverted immunodominance (1). However, FV-driven terminal exhaustion of virus-specific effector $CD8^+$ T cells may occur at the population level, because the failure to produce IFN-γ upon restimulation was observed in the entire population of Ag-experienced $CD8^+$ T cells in FV-infected mice, not just in the cells specific for the

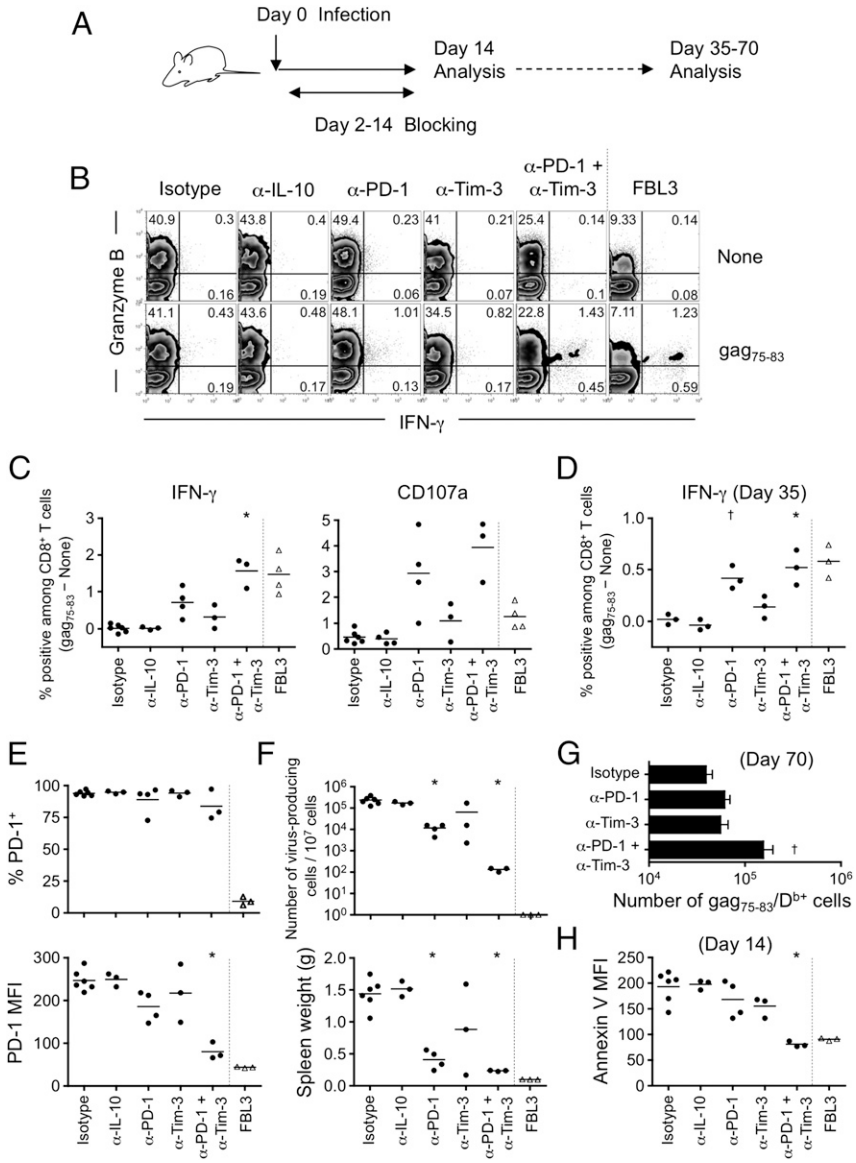

FIGURE 8. Simultaneous blockade of PD-1 and Tim-3 pathways during priming/differentiation phase rescues $CD8^+$ T cells in FV-infected mice from terminal exhaustion. *A*, Protocol for receptor blockade at the early phase of FV infection. Mice were treated with isotype-matched control IgG, anti–IL-10, anti–PD-1, anti–Tim-3, or anti–PD-1 plus anti–Tim-3 between days 2–14 postinfection/injection. Spleen cells were harvested at day 14 (*B–F*, *H*). Some groups of mice were followed up to 10 wk postinfection/injection. *B* and *C*, Fourteen days postinfection/injection, splenocytes were stimulated in vitro with $gag_{75–83}$ peptide or left unstimulated, and the intracellular expression of IFN-γ and granzyme B and surface expression of CD107a were measured by flow cytometry. *B*, Representative staining patterns for granzyme B and IFN-γ of $CD8^+$ T cells. The numbers indicate the percentage of cells gated in each quadrant. *C* and *D*, Ag-induced increase in the percentages of IFN-γ^+ and $CD107a^+$ cells among $CD8^+$ T cells at day 14 (*C*) or day 35 (*D*). *E*, The expression of PD-1 was assessed on $gag_{75–83}/D^{b+}$ $CD8^+$ T cells at day 14. *F*, The numbers of FV-producing infectious centers among 10^7 splenocytes (*upper panel*) and spleen weight (*lower panel*) in each group of mice at day 14. *G*, Actual numbers of $gag_{75–83}/D^{b+}$ $CD8^+$ T cells in the spleen at day 70. *H*, Mean fluorescence intensity of Annexin V on $gag_{75–83}/D^{b+}$ $CD8^+$ T cells at day 14. All data are representative of two independent experiments with essentially the same results. *C*, *E*, *F*, and *H*, The statistical significance of the difference in mean of each Ab-treated group from that of the control group was examined by *t* test with Bonferroni correction. $*p < \alpha\ (n = 4) = 0.0127$. *D* and *G*, $*p < 0.001$; $^{\dagger}p < 0.01$ by one-way ANOVA with Dunnett posttests against isotype control.

immunodominant gag epitope. This global nonresponsiveness of Ag-specific $CD8^+$ T cells is consistent with the previous finding that FV-infected mice were incapable of rejecting tumor cells that express FV-related epitopes, although these mice still have an ability to reject other tumor cells that express FV-unrelated epitopes (49).

The most notable feature of these dysfunctional effector $CD8^+$ T cells is the excessive expression of multiple inhibitory receptors that can negatively regulate the $CD8^+$ T cell function, such as PD-1, Tim-3, LAG-3, and CTLA-4. PD-1 has been identified as a major cell-surface inhibitory receptor capable of regulating $CD8^+$ and $CD4^+$ T cell exhaustion in mice, as well as in humans and nonhuman primates (50). Tim-3 and CTLA-4 were recently found to be overexpressed on HIV- and hepatitis C virus-specific $CD8^+$ and $CD4^+$ T cells and to act to suppress effector functions of activated T cells (11–13, 51). Upregulation of LAG-3 was also shown to correlate with the impaired effector functions and exhaustion of $CD8^+$ T cells (10, 52, 53). In addition to these inhibitory receptors, it was demonstrated that a variety of other inhibitory receptors were expressed on exhausted $CD8^+$ T cells in chronic virus infections, and the increased levels of expression were critically associated with the severity of infection and the lower functionality of $CD8^+$ T cells (10). Although the precise inhibitory mechanisms of each individual pathway are unclear, some inhibitory receptors, such as Tim-3, LAG-3, and CTLA4, are known to negatively regulate $CD8^+$ T cell function cooperatively with PD-1, because combined blockade of these inhibitory receptors, along with the PD-1/PD-L1 pathway, synergistically improved $CD8^+$ T cell responses (10–13). Based on the present observations, Ag-specific effector $CD8^+$ T cells in FV-infected mice seemed to be undergoing unusually rapid and extremely severe exhaustion. This was further confirmed by the current observation that combined blockade of PD-1 and Tim-3 during the memory phase had no effect in reinvigorating already exhausted $CD8^+$ T cells. The data obtained by using the model of nonpathogenic F-MuLV infection clearly demonstrated that acute SFFV-mediated pathogenesis was responsible for the rapid expression of multiple inhibitory receptors that cause unexpectedly rapid terminal exhaustion of effector $CD8^+$ T cells in FV-infected animals.

There has been considerable evidence that the initial viral load inversely correlates with the functionality of Ag-specific $CD8^+$ T cells (10, 54, 55). Recently, a combined in situ tetramer staining and in situ hybridization approach showed that relative rates of increase in Ag-specific effector $CD8^+$ T cells and virally infected targets during the early stage predict the outcome of viral infection (56). For example, LCMV clone 13 preferentially infects fibroblastic reticular cells,

which enables this clone to spread and replicate tremendously faster than LCMV-Armstrong, thereby exceeding the capacity of initial immune response to reduce the basic rate of replication. Moreover, fibroblastic reticular cells express high levels of PD-L1 soon after LCMV clone 13 infection, resulting in the debilitated proliferation and function of virus-specific $CD8^+$ T cells (57). These observations strikingly resemble the early events in FV infection, which is represented by the rapid expansion of virus-infected, $PD\text{-}L1^{Hi}$ erythroblasts and rapid exhaustion of $CD8^+$ T cells, although the severity of virus infection and $CD8^+$ T cell exhaustion between these models differs in degree. Considering that $CD8^+$ T cells upregulate inhibitory molecules at very early stages under the tolerogenic environment and that the negative signals provided at this stage have a profound impact on the early fate-decision of $CD8^+$ T cells (44, 58), prevention of the potential negative signals during the priming/differentiation phase is rational for rescuing virus-specific $CD8^+$ T cells from terminal exhaustion and for the effective elimination of virus-infected cells, as we successfully demonstrated in the current study.

One of the key findings from the current study is that severe FV-specific effector $CD8^+$ T cell dysfunction seemingly occurred, irrespectively of increased Treg cell numbers or functions. In fact, the suppressive ability of Treg cells did not differ between FV infection and FBL3 injection, despite the fact that the latter did not induce $CD8^+$ T cell exhaustion. Several studies have shown that FV infection results in a slight increase in the number and suppressive ability of Treg cells during the chronic phase (24, 25, 59); however, the precise role of FV-induced Treg cells in inducing the dysfunction of FV-specific $CD8^+$ T cells in vivo has not been directly elucidated. In fact, previous evidence for the involvement of Treg cells in the $CD8^+$ T cell dysfunction in vivo is based entirely on the adoptive transfer approach, in which the abilities to secrete effector cytokines were determined by using TCR-transgenic $CD8^+$ T cells that had been transferred into FV-infected animals at different stages [e.g., acute phase versus memory phase (24)]. However, these studies did not take into consideration the possible impact of different Ag/inflammation levels at the time of transfer on the priming of TCR transgenic $CD8^+$ T cells and the subsequent acquisition of effector function. The contribution of Treg cell-mediated suppression to the dysfunction of FV-specific $CD8^+$ T cells in vivo was also demonstrated by depletion of total Treg cells (24, 60). However, all animals have naturally occurring Treg (nTreg) cells that confer basal suppression of effector cell functions; the depletion of nTreg cells results in the induction of autoimmune and/or inflammatory diseases, which are associated with enhanced autoreactive cellular immune responses (61). Therefore, it is common that total Treg cell depletion in mice results in stronger cellular immune responses than do those in Treg cell-competent mice, and this could be observed with any kind of infection (62, 63). A strategy to deplete virus-induced Treg cells alone, without affecting the numbers and functions of nTreg cells, would be necessary to precisely determine the role of induced Treg cells in vivo, which has never been demonstrated. Thus, it is unknown whether FV-induced Treg cells have any roles in inducing FV-specific $CD8^+$ T cell dysfunction. In addition, because FV-infected animals are capable of mounting a $CD8^+$ T cell response against FV-unrelated tumor cells (49), the severe $CD8^+$ T cell dysfunction seems to occur in an Ag-dependent manner. Because Treg cells seem to suppress a broad spectrum of effector cells, it is unlikely that virus-induced Treg cells provide a selective contribution to the FV-specific $CD8^+$ T cell dysfunction. Moreover, direct cell-to-cell interaction is required for Treg cells from FV-infected mice to exert suppressive activity on $CD8^+$ T cells (59), and Treg cell-mediated suppression of $CD8^+$ T cell function in vivo is known to be reversible (64). These facts strongly support our conclusions on the rather minor role of Treg cells in inducing FV-specific $CD8^+$ T cell dysfunction, because the opportunity for Treg cells to interact with virus-specific $CD8^+$ T cells in FV-infected mice must be lower than that in FBL3-injected mice because of the presence of expanded erythroblasts as potential interceptors. Considering the current observations that Ag-specific $CD8^+$ T cells rapidly succumbed to terminal exhaustion in the early phase of FV infection and could not be reinvigorated, memory $CD8^+$ T cell dysfunction that has been observed in FV-infected animals may be better explained as a consequence of the currently observed premature terminal exhaustion of effector $CD8^+$ T cells rather than by Treg cell-mediated suppression.

Another issue to be considered is the possible requirement of virus-specific effector $CD8^+$ T cells for the control of FV infection. It has been believed that FV-specific $CD8^+$ T cells initially acquire effector functions during the early phase of infection, based mainly on the observation of their significant expression of granzyme B (25). However, our results draw attention to the importance of determining the responsiveness to restimulation as an indicator of $CD8^+$ T cell functionality, which is severely compromised in FV-infected mice. Another piece of evidence for the functionality of FV-specific effector $CD8^+$ T cells also relies on the approach of using supraphysiological numbers of TCR-transgenic $CD8^+$ T cells specific for the gag epitope (24). However, we clarified the nonresponsiveness of effector $CD8^+$ T cells by focusing on the endogenous FV-specific $CD8^+$ T cells induced in FV-infected mice. Because the optimal induction of functionally competent FV-specific $CD8^+$ T cell responses by early blockade of inhibitory receptors significantly improved the virus control and led to diminished FV-induced splenomegaly, it is reasonable to conclude that FV infection results in the generation of virus-specific effector $CD8^+$ T cells that are functionally impaired. One question is whether virus-specific $CD8^+$ T cells contribute to the early control of FV in vivo. Although previous studies demonstrated that the depletion of $CD8^+$ T cells significantly accelerated the acute splenomegaly (65–67), the FV stock used in these studies had been contaminated with LDV, a potent suppressor of $CD8^+$ T cell responses (27). Using the LDV-free FV stock, we confirmed an exacerbated acute splenomegaly in $CD8^+$ T cell-depleted animals upon FV infection (S. Takamura, S. Tsuji-Kawahara, and M. Miyazawa, unpublished observations), which seems to conflict with our current observations regarding the early loss of FV-specific $CD8^+$ T cell function. One potential explanation is that a short lag exists between the functional maturation and the subsequent exhaustion of $CD8^+$ T cells in the early stage of FV infection, during which FV-infected cells are at least partially eliminated by effector $CD8^+$ T cells. Alternatively, because weak, but spontaneous, degranulation was observed on granzyme B^+CD8^+ T cells in FV-infected, but not FBL3-injected, mice, the expanded FV-infected erythroblasts that dominated in the spleen can be eliminated in an Ag-independent manner. We are currently investigating these possibilities.

Overall, the data presented in this article indicate that FV, but not F-MuLV, silences antiviral $CD8^+$ T cell responses during the early phase of infection by inducing the rapid and high expression of multiple inhibitory receptors, leading to irreversible terminal exhaustion. These findings have to be considered a newly recognized strategy for FV to escape from acute $CD8^+$ T cell responses. Finally, manipulation of $CD8^+$ T cell exhaustion by early blockade of multiple inhibitory receptors would be necessary to control the pathogens, such as HIV, that exhibit widespread terminal exhaustion of $CD8^+$ T cells.

Acknowledgments

We thank Nobuharu Kurashimo for technical assistance with flow cytometry and Dr. Eiji Kajiwara, Dr. Yoshiyuki Hakata, and J. Brian Dowell for critically reviewing the manuscript.

Disclosures

The authors have no financial conflicts of interest.

References

1. Wherry, E. J., J. N. Blattman, K. Murali-Krishna, R. van der Most, and R. Ahmed. 2003. Viral persistence alters CD8 T-cell immunodominance and tissue distribution and results in distinct stages of functional impairment. *J. Virol.* 77: 4911–4927.
2. Barber, D. L., E. J. Wherry, D. Masopust, B. Zhu, J. P. Allison, A. H. Sharpe, G. J. Freeman, and R. Ahmed. 2006. Restoring function in exhausted CD8 T cells during chronic viral infection. *Nature* 439: 682–687.
3. Petrovas, C., D. A. Price, J. Mattapallil, D. R. Ambrozak, C. Geldmacher, V. Cecchinato, M. Vaccari, E. Tryniszewska, E. Gostick, M. Roederer, et al. 2007. SIV-specific CD8+ T cells express high levels of PD1 and cytokines but have impaired proliferative capacity in acute and chronic SIVmac251 infection. *Blood* 110: 928–936.
4. Zhang, J. Y., Z. Zhang, X. Wang, J. L. Fu, J. Yao, Y. Jiao, L. Chen, H. Zhang, J. Wei, L. Jin, et al. 2007. PD-1 up-regulation is correlated with HIV-specific memory CD8+ T-cell exhaustion in typical progressors but not in long-term nonprogressors. *Blood* 109: 4671–4678.
5. Velu, V., S. Kannanganat, C. Ibegbu, L. Chennareddi, F. Villinger, G. J. Freeman, R. Ahmed, and R. R. Amara. 2007. Elevated expression levels of inhibitory receptor programmed death 1 on simian immunodeficiency virus-specific CD8 T cells during chronic infection but not after vaccination. *J. Virol.* 81: 5819–5828.
6. Trautmann, L., L. Janbazian, N. Chomont, E. A. Said, S. Gimmig, B. Bessette, M. R. Boulassel, E. Delwart, H. Sepulveda, R. S. Balderas, et al. 2006. Upregulation of PD-1 expression on HIV-specific CD8+ T cells leads to reversible immune dysfunction. *Nat. Med.* 12: 1198–1202.
7. Day, C. L., D. E. Kaufmann, P. Kiepiela, J. A. Brown, E. S. Moodley, S. Reddy, E. W. Mackey, J. D. Miller, A. J. Leslie, C. DePierres, et al. 2006. PD-1 expression on HIV-specific T cells is associated with T-cell exhaustion and disease progression. *Nature* 443: 350–354.
8. Nakamoto, N., D. E. Kaplan, J. Coleclough, Y. Li, M. E. Valiga, M. Kaminski, A. Shaked, K. Olthoff, E. Gostick, D. A. Price, G. J. Freeman, E. J. Wherry, and K. M. Chang. 2008. Functional restoration of HCV-specific CD8 T cells by PD-1 blockade is defined by PD-1 expression and compartmentalization. *Gastroenterology* 134: 1927–1937.e1–2.
9. Blackburn, S. D., H. Shin, G. J. Freeman, and E. J. Wherry. 2008. Selective expansion of a subset of exhausted CD8 T cells by αPD-L1 blockade. *Proc. Natl. Acad. Sci. USA* 105: 15016–15021.
10. Blackburn, S. D., H. Shin, W. N. Haining, T. Zou, C. J. Workman, A. Polley, M. R. Betts, G. J. Freeman, D. A. Vignali, and E. J. Wherry. 2009. Coregulation of CD8+ T cell exhaustion by multiple inhibitory receptors during chronic viral infection. *Nat. Immunol.* 10: 29–37.
11. Jones, R. B., L. C. Ndhlovu, J. D. Barbour, P. M. Sheth, A. R. Jha, B. R. Long, J. C. Wong, M. Satkunarajah, M. Schweneker, J. M. Chapman, et al. 2008. Tim-3 expression defines a novel population of dysfunctional T cells with highly elevated frequencies in progressive HIV-1 infection. *J. Exp. Med.* 205: 2763–2779.
12. Kaufmann, D. E., D. G. Kavanagh, F. Pereyra, J. J. Zaunders, E. W. Mackey, T. Miura, S. Palmer, M. Brockman, A. Rathod, A. Piechocka-Trocha, et al. 2007. Upregulation of CTLA-4 by HIV-specific CD4+ T cells correlates with disease progression and defines a reversible immune dysfunction. *Nat. Immunol.* 8: 1246–1254.
13. Nakamoto, N., H. Cho, A. Shaked, K. Olthoff, M. E. Valiga, M. Kaminski, E. Gostick, D. A. Price, G. J. Freeman, E. J. Wherry, and K. M. Chang. 2009. Synergistic reversal of intrahepatic HCV-specific CD8 T cell exhaustion by combined PD-1/CTLA-4 blockade. *PLoS Pathog.* 5: e1000313.
14. Ha, S. J., S. N. Mueller, E. J. Wherry, D. L. Barber, R. D. Aubert, A. H. Sharpe, G. J. Freeman, and R. Ahmed. 2008. Enhancing therapeutic vaccination by blocking PD-1-mediated inhibitory signals during chronic infection. *J. Exp. Med.* 205: 543–555.
15. Miyazawa, M., S. Tsuji-Kawahara, and Y. Kanari. 2008. Host genetic factors that control immune responses to retrovirus infections. *Vaccine* 26: 2981–2996.
16. Albritton, L. M., L. Tseng, D. Scadden, and J. M. Cunningham. 1989. A putative murine ecotropic retrovirus receptor gene encodes a multiple membrane-spanning protein and confers susceptibility to virus infection. *Cell* 57: 659–666.
17. Kim, J. W., E. I. Closs, L. M. Albritton, and J. M. Cunningham. 1991. Transport of cationic amino acids by the mouse ecotropic retrovirus receptor. *Nature* 352: 725–728.
18. Wang, H., M. P. Kavanaugh, R. A. North, and D. Kabat. 1991. Cell-surface receptor for ecotropic murine retroviruses is a basic amino-acid transporter. *Nature* 352: 729–731.
19. Robertson, M. N., M. Miyazawa, S. Mori, B. Caughey, L. H. Evans, S. F. Hayes, and B. Chesebro. 1991. Production of monoclonal antibodies reactive with a denatured form of the Friend murine leukemia virus gp70 envelope protein: use in a focal infectivity assay, immunohistochemical studies, electron microscopy and western blotting. *J. Virol. Methods* 34: 255–271.
20. Chesebro, B., M. Miyazawa, and W. J. Britt. 1990. Host genetic control of spontaneous and induced immunity to Friend murine retrovirus infection. *Annu. Rev. Immunol.* 8: 477–499.
21. Kabat, D. 1989. Molecular biology of Friend viral erythroleukemia. *Curr. Top. Microbiol. Immunol.* 148: 1–42.
22. Chesebro, B., M. Bloom, K. Wehrly, and J. Nishio. 1979. Persistence of infectious Friend virus in spleens of mice after spontaneous recovery from virus-induced erythroleukemia. *J. Virol.* 32: 832–837.
23. Zanovello, P., D. Collavo, F. Ronchese, A. De Rossi, G. Biasi, and L. Chieco-Bianchi. 1984. Virus-specific T cell response prevents lymphoma development in mice infected by intrathymic inoculation of Moloney leukaemia virus (M-MuLV). *Immunology* 51: 9–16.
24. Dittmer, U., H. He, R. J. Messer, S. Schimmer, A. R. Olbrich, C. Ohlen, P. D. Greenberg, I. M. Stromnes, M. Iwashiro, S. Sakaguchi, et al. 2004. Functional impairment of CD8(+) T cells by regulatory T cells during persistent retroviral infection. *Immunity* 20: 293–303.
25. Zelinskyy, G., A. R. Kraft, S. Schimmer, T. Arndt, and U. Dittmer. 2006. Kinetics of CD8+ effector T cell responses and induced CD4+ regulatory T cell responses during Friend retrovirus infection. *Eur. J. Immunol.* 36: 2658–2670.
26. Zelinskyy, G., S. J. Robertson, S. Schimmer, R. J. Messer, K. J. Hasenkrug, and U. Dittmer. 2005. CD8+ T-cell dysfunction due to cytolytic granule deficiency in persistent Friend retrovirus infection. *J. Virol.* 79: 10619–10626.
27. Robertson, S. J., C. G. Ammann, R. J. Messer, A. B. Carmody, L. Myers, U. Dittmer, S. Nair, N. Gerlach, L. H. Evans, W. A. Cafruny, and K. J. Hasenkrug. 2008. Suppression of acute anti-Friend virus CD8+ T-cell responses by coinfection with lactate dehydrogenase-elevating virus. *J. Virol.* 82: 408–418.
28. Takeda, E., S. Tsuji-Kawahara, M. Sakamoto, M. A. Langlois, M. S. Neuberger, C. Rada, and M. Miyazawa. 2008. Mouse APOBEC3 restricts Friend leukemia virus infection and pathogenesis in vivo. *J. Virol.* 82: 10998–11008.
29. Hirama, T., S. Takeshita, Y. Matsubayashi, M. Iwashiro, T. Masuda, K. Kuribayashi, Y. Yoshida, and H. Yamagishi. 1991. Conserved V(D)J junctional sequence of cross-reactive cytotoxic T cell receptor idiotype and the effect of a single amino acid substitution. *Eur. J. Immunol.* 21: 483–488.
30. Hikono, H., J. E. Kohlmeier, S. Takamura, S. T. Wittmer, A. D. Roberts, and D. L. Woodland. 2007. Activation phenotype, rather than central- or effector-memory phenotype, predicts the recall efficacy of memory CD8+ T cells. *J. Exp. Med.* 204: 1625–1636.
31. Kawabata, H., A. Niwa, S. Tsuji-Kawahara, H. Uenishi, N. Iwanami, H. Matsukuma, H. Abe, N. Tabata, H. Matsumura, and M. Miyazawa. 2006. Peptide-induced immune protection of CD8+ T cell-deficient mice against Friend retrovirus-induced disease. *Int. Immunol.* 18: 183–198.
32. Myers, L., R. J. Messer, A. B. Carmody, and K. J. Hasenkrug. 2009. Tissue-specific abundance of regulatory T cells correlates with CD8+ T cell dysfunction and chronic retrovirus loads. *J. Immunol.* 183: 1636–1643.
33. Yamazaki, T., H. Akiba, A. Koyanagi, M. Azuma, H. Yagita, and K. Okumura. 2005. Blockade of B7-H1 on macrophages suppresses CD4+ T cell proliferation by augmenting IFN-gamma-induced nitric oxide production. *J. Immunol.* 175: 1586–1592.
34. Oikawa, T., Y. Kamimura, H. Akiba, H. Yagita, K. Okumura, H. Takahashi, M. Zeniya, H. Tajiri, and M. Azuma. 2006. Preferential involvement of Tim-3 in the regulation of hepatic CD8+ T cells in murine acute graft-versus-host disease. *J. Immunol.* 177: 4281–4287.
35. Aramaki, O., F. Inoue, T. Takayama, M. Shimazu, M. Kitajima, Y. Ikeda, K. Okumura, H. Yagita, N. Shirasugi, and M. Niimi. 2005. Interleukin-10 but not transforming growth factor-beta is essential for generation and suppressor function of regulatory cells induced by intratracheal delivery of alloantigen. *Transplantation* 79: 568–576.
36. Nakayama, M., H. Akiba, K. Takeda, Y. Kojima, M. Hashiguchi, M. Azuma, H. Yagita, and K. Okumura. 2009. Tim-3 mediates phagocytosis of apoptotic cells and cross-presentation. *Blood* 113: 3821–3830.
37. Chang, W. S., J. Y. Kim, Y. J. Kim, Y. S. Kim, J. M. Lee, M. Azuma, H. Yagita, and C. Y. Kang. 2008. Cutting Edge: Programmed death-1/programmed death ligand 1 interaction regulates the induction and maintenance of invariant NKT cell anergy. *J. Immunol.* 181: 6707–6710.
38. Martin-Orozco, N., Y. H. Wang, H. Yagita, and C. Dong. 2006. Cutting Edge: Programmed death (PD) ligand-1/PD-1 interaction is required for CD8+ T cell tolerance to tissue antigens. *J. Immunol.* 177: 8291–8295.
39. Chen, W., H. Qin, B. Chesebro, and M. A. Cheever. 1996. Identification of a gag-encoded cytotoxic T-lymphocyte epitope from FBL-3 leukemia shared by Friend, Moloney, and Rauscher murine leukemia virus-induced tumors. *J. Virol.* 70: 7773–7782.
40. Mintern, J. D., C. Guillonneau, F. R. Carbone, P. C. Doherty, and S. J. Turner. 2007. Cutting Edge: Tissue-resident memory CTL down-regulate cytolytic molecule expression following virus clearance. *J. Immunol.* 179: 7220–7224.
41. Wherry, E. J., S. J. Ha, S. M. Kaech, W. N. Haining, S. Sarkar, V. Kalia, S. Subramaniam, J. N. Blattman, D. L. Barber, and R. Ahmed. 2007. Molecular signature of CD8+ T cell exhaustion during chronic viral infection. *Immunity* 27: 670–684.
42. Sharpe, A. H., E. J. Wherry, R. Ahmed, and G. J. Freeman. 2007. The function of programmed cell death 1 and its ligands in regulating autoimmunity and infection. *Nat. Immunol.* 8: 239–245.
43. Giles, C. M., M. J. Walport, J. David, and C. Darke. 1987. Expression of MHC class I determinants on erythrocytes of SLE patients. *Clin. Exp. Immunol.* 69: 368–374.
44. Goldberg, M. V., C. H. Maris, E. L. Hipkiss, A. S. Flies, L. Zhen, R. M. Tuder, J. F. Grosso, T. J. Harris, D. Getnet, K. A. Whartenby, et al. 2007. Role of PD-1 and its ligand, B7-H1, in early fate decisions of CD8 T cells. *Blood* 110: 186–192.
45. Sugahara, D., S. Tsuji-Kawahara, and M. Miyazawa. 2004. Identification of a protective CD4+ T-cell epitope in p15gag of Friend murine leukemia virus and role of the MA protein targeting the plasma membrane in immunogenicity. *J. Virol.* 78: 6322–6334.
46. Brooks, D. G., M. J. Trifilo, K. H. Edelmann, L. Teyton, D. B. McGavern, and M. B. Oldstone. 2006. Interleukin-10 determines viral clearance or persistence in vivo. *Nat. Med.* 12: 1301–1309.
47. Brooks, D. G., S. J. Ha, H. Elsaesser, A. H. Sharpe, G. J. Freeman, and M. B. Oldstone. 2008. IL-10 and PD-L1 operate through distinct pathways to suppress T-cell activity during persistent viral infection. *Proc. Natl. Acad. Sci. USA* 105: 20428–20433.

48. Ejrnaes, M., C. M. Filippi, M. M. Martinic, E. M. Ling, L. M. Togher, S. Crotty, and M. G. von Herrath. 2006. Resolution of a chronic viral infection after interleukin-10 receptor blockade. *J. Exp. Med.* 203: 2461–2472.
49. Iwashiro, M., R. J. Messer, K. E. Peterson, I. M. Stromnes, T. Sugie, and K. J. Hasenkrug. 2001. Immunosuppression by CD4+ regulatory T cells induced by chronic retroviral infection. *Proc. Natl. Acad. Sci. USA* 98: 9226–9230.
50. Keir, M. E., M. J. Butte, G. J. Freeman, and A. H. Sharpe. 2008. PD-1 and its ligands in tolerance and immunity. *Annu. Rev. Immunol.* 26: 677–704.
51. Golden-Mason, L., B. E. Palmer, N. Kassam, L. Townshend-Bulson, S. Livingston, B. McMahon, N. Castelblanco, V. Kuchroo, D. R. Gretch, and H. R. Rosen. 2009. Negative immune regulator Tim-3 is overexpressed in hepatitis C infection and its blockade rescues dysfunctional CD4+ and CD8+ T cells. *J. Virol.* 83: 9122–9130.
52. Grosso, J. F., C. C. Kelleher, T. J. Harris, C. H. Maris, E. L. Hipkiss, A. De Marzo, R. Anders, G. Netto, D. Getnet, T. C. Bruno, et al. 2007. LAG-3 regulates CD8+ T cell accumulation and effector function in murine self- and tumor-tolerance systems. *J. Clin. Invest.* 117: 3383–3392.
53. Grosso, J. F., M. V. Goldberg, D. Getnet, T. C. Bruno, H. R. Yen, K. J. Pyle, E. Hipkiss, D. A. Vignali, D. M. Pardoll, and C. G. Drake. 2009. Functionally distinct LAG-3 and PD-1 subsets on activated and chronically stimulated CD8 T cells. *J. Immunol.* 182: 6659–6669.
54. Sad, S., R. Dudani, K. Gurnani, M. Russell, H. van Faassen, B. Finlay, and L. Krishnan. 2008. Pathogen proliferation governs the magnitude but compromises the function of CD8 T cells. *J. Immunol.* 180: 5853–5861.
55. Streeck, H., Z. L. Brumme, M. Anastario, K. W. Cohen, J. S. Jolin, A. Meier, C. J. Brumme, E. S. Rosenberg, G. Alter, T. M. Allen, et al. 2008. Antigen load and viral sequence diversification determine the functional profile of HIV-1-specific CD8+ T cells. *PLoS Med.* 5: e100.
56. Li, Q., P. J. Skinner, S. J. Ha, L. Duan, T. L. Mattila, A. Hage, C. White, D. L. Barber, L. O'Mara, P. J. Southern, et al. 2009. Visualizing antigen-specific and infected cells in situ predicts outcomes in early viral infection. *Science* 323: 1726–1729.
57. Mueller, S. N., M. Matloubian, D. M. Clemens, A. H. Sharpe, G. J. Freeman, S. Gangappa, C. P. Larsen, and R. Ahmed. 2007. Viral targeting of fibroblastic reticular cells contributes to immunosuppression and persistence during chronic infection. *Proc. Natl. Acad. Sci. USA* 104: 15430–15435.
58. Tsushima, F., S. Yao, T. Shin, A. Flies, S. Flies, H. Xu, K. Tamada, D. M. Pardoll, and L. Chen. 2007. Interaction between B7-H1 and PD-1 determines initiation and reversal of T-cell anergy. *Blood* 110: 180–185.
59. Robertson, S. J., R. J. Messer, A. B. Carmody, and K. J. Hasenkrug. 2006. In vitro suppression of CD8+ T cell function by Friend virus-induced regulatory T cells. *J. Immunol.* 176: 3342–3349.
60. Zelinskyy, G., K. K. Dietze, Y. P. Hüsecken, S. Schimmer, S. Nair, T. Werner, K. Gibbert, O. Kershaw, A. D. Gruber, T. Sparwasser, and U. Dittmer. 2009. The regulatory T-cell response during acute retroviral infection is locally defined and controls the magnitude and duration of the virus-specific cytotoxic T-cell response. *Blood* 114: 3199–3207.
61. Sakaguchi, S., M. Ono, R. Setoguchi, H. Yagi, S. Hori, Z. Fehervari, J. Shimizu, T. Takahashi, and T. Nomura. 2006. Foxp3+ CD25+ CD4+ natural regulatory T cells in dominant self-tolerance and autoimmune disease. *Immunol. Rev.* 212: 8–27.
62. Haeryfar, S. M., R. J. DiPaolo, D. C. Tscharke, J. R. Bennink, and J. W. Yewdell. 2005. Regulatory T cells suppress CD8+ T cell responses induced by direct priming and cross-priming and moderate immunodominance disparities. *J. Immunol.* 174: 3344–3351.
63. Chaudhry, A., D. Rudra, P. Treuting, R. M. Samstein, Y. Liang, A. Kas, and A. Y. Rudensky. 2009. CD4+ regulatory T cells control TH17 responses in a Stat3-dependent manner. *Science* 326: 986–991.
64. Mempel, T. R., M. J. Pittet, K. Khazaie, W. Weninger, R. Weissleder, H. von Boehmer, and U. H. von Andrian. 2006. Regulatory T cells reversibly suppress cytotoxic T cell function independent of effector differentiation. *Immunity* 25: 129–141.
65. Hasenkrug, K. J. 1999. Lymphocyte deficiencies increase susceptibility to Friend virus-induced erythroleukemia in Fv-2 genetically resistant mice. *J. Virol.* 73: 6468–6473.
66. Hasenkrug, K. J., D. M. Brooks, and U. Dittmer. 1998. Critical role for CD4(+) T cells in controlling retrovirus replication and spread in persistently infected mice. *J. Virol.* 72: 6559–6564.
67. Robertson, M. N., G. J. Spangrude, K. Hasenkrug, L. Perry, J. Nishio, K. Wehrly, and B. Chesebro. 1992. Role and specificity of T-cell subsets in spontaneous recovery from Friend virus-induced leukemia in mice. *J. Virol.* 66: 3271–3277.